NACA RM No. A7F25

NACA

RESEARCH MEMORANDUM

15 DEC 1947

A COMPARISON WITH FLIGHT DATA OF VERTICAL-TAIL LOADS IN VARIOUS MANEUVERS ESTIMATED FROM SIDESLIP ANGLES AND RUDDER DEFLECTIONS

By

Howard L. Turner

Ames Aeronautical Laboratory
Moffett Field, Calif.

NATIONAL ADVISORY COMMITTEE
FOR AERONAUTICS

WASHINGTON

December 11, 1947

NACA RM No. A7F25

NATIONAL ADVISORY COMMITTEE FOR AERONAUTICS

RESEARCH MEMORANDUM

A COMPARISON WITH FLIGHT DATA OF VERTICAL-TAIL LOADS IN VARIOUS MANEUVERS ESTIMATED FROM SIDESLIP ANGLES AND RUDDER DEFLECTIONS

By Howard L. Turner

SUMMARY

A comparison is made of the vertical-tail loads determined from pressure-distribution measurements in flight in various maneuvers with the corresponding vertical-tail loads calculated, using the values of sideslip angles and rudder deflections as measured during the various maneuvers. The maneuvers investigated included slow rolls, steady sideslips, fishtails, and rolling pull-outs. The loads were calculated only for the sideslip angles and rudder deflections corresponding to the maximum measured load in each maneuver. For the maneuvers investigated, the calculated loads were found to be conservative by approximately 16 percent as compared with the experimental loads. The sources of error in the methods of estimating some of these aerodynamic parameters and their effects on the vertical-tail load computations are discussed briefly.

INTRODUCTION

In several of the more recently proposed methods for computing critical vertical-tail loads, it is necessary, in a given type of maneuver, to determine the values of sideslip angle β, the rudder angle δ_r, and the yawing velocity r, in order to predict the total vertical-tail loads. Methods for predicting these values analytically for various types of maneuvers are presented in references 1, 2, and 3, although in some of these cases partial verification of the general method of computing vertical-tail loads is provided by comparing computed results with values from flight tests, there still remains some uncertainty as to the accuracy with

which the total vertical-tail loads may be predicted using available means for estimating aerodynamic parameters from airplane geometry alone.

In order to provide data to further substantiate the validity of one step in the prediction of tail loads, flight tests were conducted on a propeller-driven fighter-type airplane in which vertical-tail loads were measured, by orifices on the surface of the vertical tail, in various static and dynamic maneuvers. Simultaneous values of sideslip angle, rudder deflection, and yawing velocity were also measured. From these data and the aerodynamic parameters evaluated using the vertical-tail geometry, the vertical-tail loads were computed and then compared with the corresponding loads measured in flight.

SYMBOLS

L_t total vertical-tail load, pounds (Positive when acting to the right.)

V_t true airspeed, feet per second

V_i indicated airspeed, miles per hour

$$\left\{V_i = 1703\left[\left(\frac{q_c}{P_o} + 1\right)^{0.286} - 1\right]^{\frac{1}{2}}\right\}$$

q_o free stream dynamic pressure, pounds per square foot

q_t dynamic pressure at the tail, pounds per square foot

q_c impact pressure shown by pitot-static tube, pounds per square inch

S_t vertical-tail area, square feet

l_t distance from airplane center of gravity to rudder hinge line, feet

c local vertical-tail chord, feet

P_o resultant pressure, pounds per square foot

c_n section normal-force coefficient

C_N normal-force coefficient

r yawing velocity, radians per second

β angle of sideslip, degrees (Positive when right wing forward.)

φ fin offset, from fuselage center line, degrees (Positive when leading edge to the left.)

σ angle of sidewash, degrees

δ_r rudder deflection from fin center line, degrees (Right rudder positive.)

α_t effective vertical-tail angle of attack, degrees

τ relative rudder effectiveness $\left(\frac{d\alpha_t}{d\delta_r} = \frac{\partial C_{N_t}/\partial \delta_r}{\partial C_{N_t}/\partial \alpha_t}\right)$

$\left(\frac{dC_N}{d\alpha}\right)_t$ vertical-tail lift-curve slope

$\frac{dC_{N_t}}{d\delta_r}$ slope of vertical-tail normal-force coefficient versus rudder deflection curve

TESTS, APPARATUS, AND PRECISION

The test maneuvers used in this investigation were steady sideslips, slow rolls, fishtails, and rolling pull-outs. Steady sideslips were made with power off and with normal rated power. All other maneuvers were performed with normal rated power only. All the tests were made at an average altitude of 10,000 feet.

The test vehicle used in this investigation was a single-engine, propeller-driven, fighter-type airplane. (See fig. 1.) NACA continuous-film recording instruments

were used to measure, as a function of time, the control positions, sideslip angle, yawing velocity, airspeed, altitude, and the resultant pressures over the vertical tail. Figure 2 is a side view of the vertical tail of the test airplane showing the principal dimensions and the locations of the pressure orifice stations.

The precision with which the sideslip angles and the rudder deflections were measured was believed to be $\pm\frac{1}{2}^{\circ}$. The vertical-tail loads obtained from the pressure distributions are believed to be accurate to ±3 percent for the static maneuvers and ±5 percent for the dynamic maneuvers, depending upon the magnitude of the load.

METHOD

The total aerodynamic load on the vertical tail for any static or dynamic maneuver may be given by the expression:

$$L_t = S_t q_t \left[\left(\beta + \frac{57.3 r l_t}{V_T} + \varphi + \sigma\right)\left(\frac{\partial C_N}{\partial \alpha}\right)_t + \delta_r \left(\frac{\partial C_{N_t}}{\partial \delta_r}\right)\right] \tag{1}$$

For convenience in the use of this expression, equation (1) may be written as

$$L_t = S_t q_t \left(\frac{dC_N}{d\alpha}\right)_t \alpha_t \tag{2}$$

where

$$\alpha_t = \beta + \varphi + \sigma + \frac{57.3 r l_t}{V_t} + \tau \delta_r \tag{2a}$$

where

$$\tau = \frac{\partial C_{N_t}/\partial \delta_r}{\partial C_{N_t}/\partial \alpha_t}$$

In applying these equations to the computations of vertical-tail loads, it is necessary that the methods of defining the coefficients be considered. In equation (2), the area of the vertical-tail S_t was assumed to be the area of the fin above the fin-fuselage juncture plus the movable area of the vertical tail; this assumption conforms with the convention set up in reference 4. This is the area covered by the pressure orifices as shown in figure 2. The dynamic pressure at the tail q_t was assumed to be equal to the free-stream dynamic pressure q_o. The slope of the vertical-tail lift curve was estimated from figure 3 of reference 4. The effective angle of attack of the vertical tail α_t is given by equation (2a).

In evaluating equation (2a) for the present analysis, the values of sideslip angle, rudder deflection, yawing velocity, and airspeed are those measured in flight at the time of maximum sideslip, and correspond to the maximum loading condition in the maneuvers investigated. The fin offset angle φ is fixed at 1° left of fuselage center line. The angle of sidewash, discussed in reference 4, was neglected in this report due to the lack of sufficient information for accurate estimation. The relative rudder effectiveness τ, which is based on the relative areas of the rudder, the rudder balance, and the vertical tail, was estimated from figure 4 of reference 4. Since this report deals with load conditions at the time of maximum sideslip, the increment of angle of attack due to yawing velocity may be neglected. Hence, for the purpose of this investigation, the effective vertical-tail angle of attack may be expressed as

$$\alpha_t = \beta + \varphi + \tau\delta_r \qquad (3)$$

Using the dimensions shown in figure 2, the following geometric parameters were evaluated:

$$\text{Geometric aspect ratio} = b^2/S_t = \frac{4.1^2}{19.01} = 0.884$$

Effective aspect ratio = 1.55 (0.884) = 1.37

$$S_r/S_t = \frac{9.55}{19.01} = 0.502$$

$$S_b/S_r = \frac{1.52}{9.55} = 0.159$$

These parameters were applied to figures 3 and 4 of reference 4 to establish the values of the following:

$$(dC_N/d\alpha)_t = 0.035$$

$$\tau = 0.74$$

RESULTS AND DISCUSSION

Typical pressure distributions are presented in figure 3 to show the type of data from which the experimental loads were obtained. From these pressure distributions and from similar plots not included in this report, the experimental total vertical-tail loads were evaluated. In figure 4(a) the flight-measured loads are compared with the calculated loads at various indicated airspeeds for two power conditions. Figure 4(a) indicates that, for the maneuvers investigated, the effects of power appear to be negligible, and that the calculated vertical-tail loads were approximately 16 percent greater than the corresponding flight-measured loads. This discrepancy is not too large and may be acceptable for preliminary design. However, a brief discussion of the possible sources of error entering into the tail load equation may be of some aid in interpreting these results.

In equation (2), it is seen that the accurate estimation of q_t and $\left(\frac{dC_N}{d\alpha}\right)_t$ is necessary before any conclusion can be made about the adequacy of equation (3). Although an error in q_t would effect a similar error in the values of the calculated vertical-tail loads, agreement of the power-on and power-off data of this report indicates that for the speed range and test condition investigated, the assumption of $q_t = q_o$ introduces negligible error.

The estimation of $\left(\frac{dC_N}{d\alpha}\right)_t$ by the method of reference 4 is subject to possible error, since the effective aspect ratio of the vertical tail is determined by the use of several arbitrary assumptions. Figure 5 compares the experimental vertical-tail lift-curve slope obtained from flight data with the estimated vertical-tail lift-curve slope from reference 4 for a rudder angle of approximately -3°. The experimental value of $\left(\frac{dC_N}{d\alpha}\right)_t$ of 0.030 is 13 percent less than the value of 0.035 estimated from reference 4. This difference is sufficient to account for most of the discrepancy noted between the measured and the computed vertical-tail loads. Consideration of the values of δ_r and $\beta + \varphi$ at $C_{N_t} = 0$ indicates a value of τ of about 0.80 which represents a reasonable check of the assumed value of 0.74.

Figure 6 indicates a sizeable difference between static and dynamic maneuvers in the effective angle of attack of the vertical tail due to rudder deflection, particularly in left sideslip. In an effort to determine the sensitivity of the estimated vertical-tail loads to the value of the relative rudder effectiveness τ, the computed loads were recalculated using another value of τ differing from that originally used by about 30 percent. The results of the computation are shown in figure 4(b). The estimated lift-curve slope $dC_N/d\alpha_t$ was unchanged from that used in the computation for figure 4(a). It may be seen in figures 4(a) and 4(b) that although the new value of τ somewhat reduces the difference between static and dynamic maneuvers, it does not reduce the discrepancy between flight loads and computed loads. It may be further observed that the use of $\tau = 0.5$ introduces an asymmetry in the alinement of the test data but does not reduce appreciably the over-all dispersion of the test points. However, it may be concluded that small changes in the value assigned to the parameter τ do not greatly influence the agreement obtainable between flight-measured and computed vertical-tail loads.

CONCLUSIONS

On the basis of the tests conducted on a typical fighter-type airplane, the following conclusions were reached which are probably generally applicable only to airplanes having a

tail configuration similar to that tested:

1. The effective angle of attack of the vertical tail under maximum loading conditions is adequately defined by combining the sideslip angle with the fin offset angle and the angle increment equivalent to the rudder deflection.

2. If the maximum sideslip angle and the rudder deflection at the time of maximum loading of the vertical tail are known, the maximum loads in static and dynamic maneuvers may be predicted fairly accurately. Using current methods of estimation, the calculated vertical-tail loads were found to be approximately 16 percent greater than the corresponding flight-measured loads.

3. The most important single factor in this estimation of vertical-tail loads appears to be the vertical-tail lift-curve slope. Further improvements in the accuracy of estimating the vertical-tail loads appear to be dependent upon more accurate means for estimating the vertical-tail lift-curve slope.

Ames Aeronautical Laboratory,
National Advisory Committee for Aeronautics,
Moffett Field, Calif.

REFERENCES

1. White, Maurice D.; Lomax, Harvard, and Turner, Howard L.: Sideslip Angles and Vertical-Tail Loads in Rolling Pull-Out Maneuvers. NACA TN No. 1122, 1947.

2. Gilruth, Robert R.: Analysis of Vertical-Tail Loads in Rolling Pull-Out Maneuvers. NACA CB No. L4H14, 1944.

3. Posner, E. C.: Airplane Maneuvering Loads. Jour. Aero. Sci., vol. 13, no. 6, June 1946, pp. 325-331.

4. Pass, H. R.: Analysis of Wind-Tunnel Data on Directional Stability and Control. NACA TN No. 775, 1940.

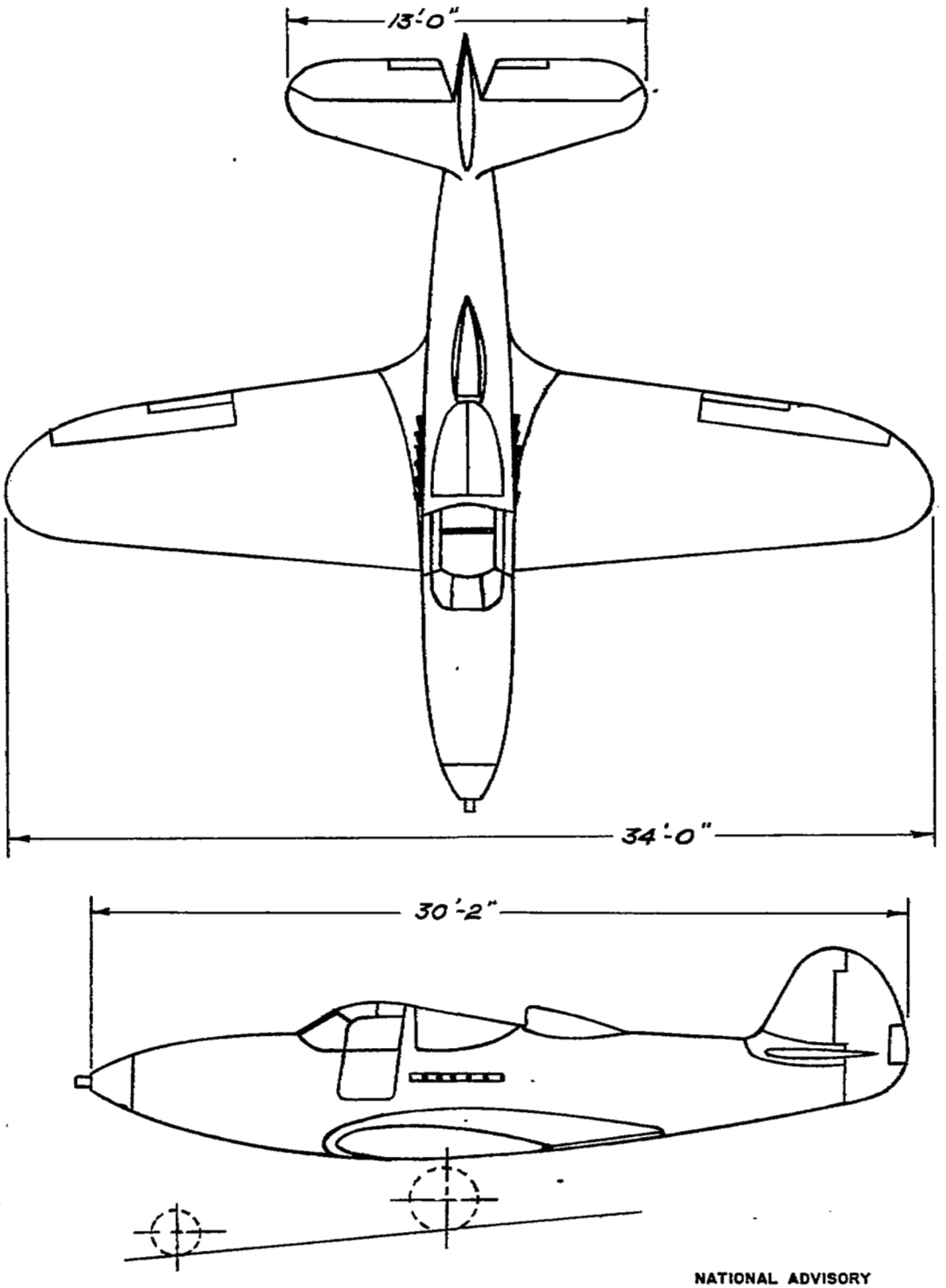

Figure 1.- Plan and side views of test airplane.

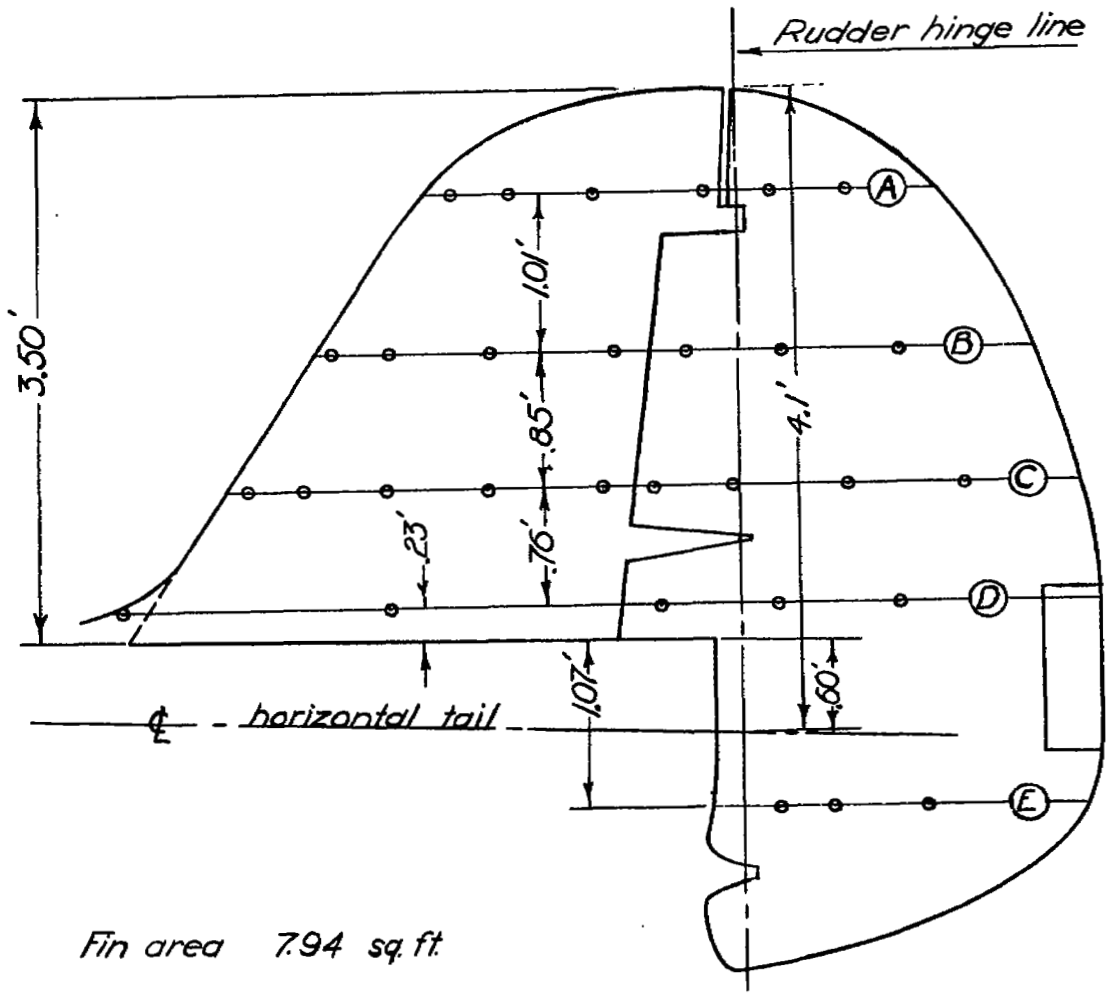

Fin area 7.94 sq. ft.

Balance area (ahead hinge line) 1.52 sq. ft.

Rudder area (aft hinge line) 9.55 sq. ft.

Total vertical tail area 19.01 sq. ft.

Effective span (tip to center line horizontal tail) 4.1 ft.

NATIONAL ADVISORY COMMITTEE FOR AERONAUTICS

Figure 2.- Vertical-tail of the test airplane showing the location of the pressure orifices.

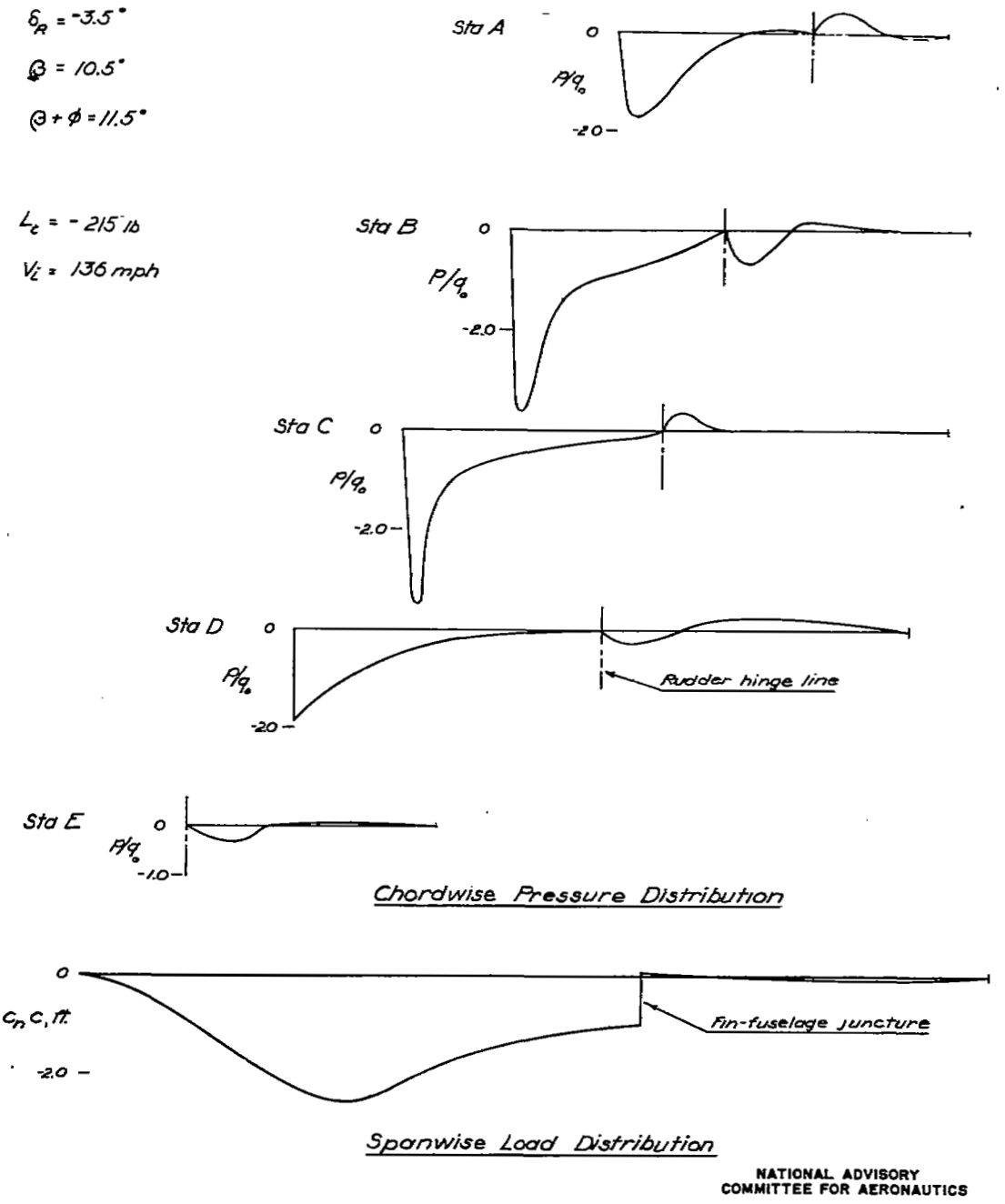

(a) Steady-sideslip maneuver

Figure 3.- Typical vertical-tail chordwise pressure distributions and spanwise load distributions in various maneuvers, normal rated power.

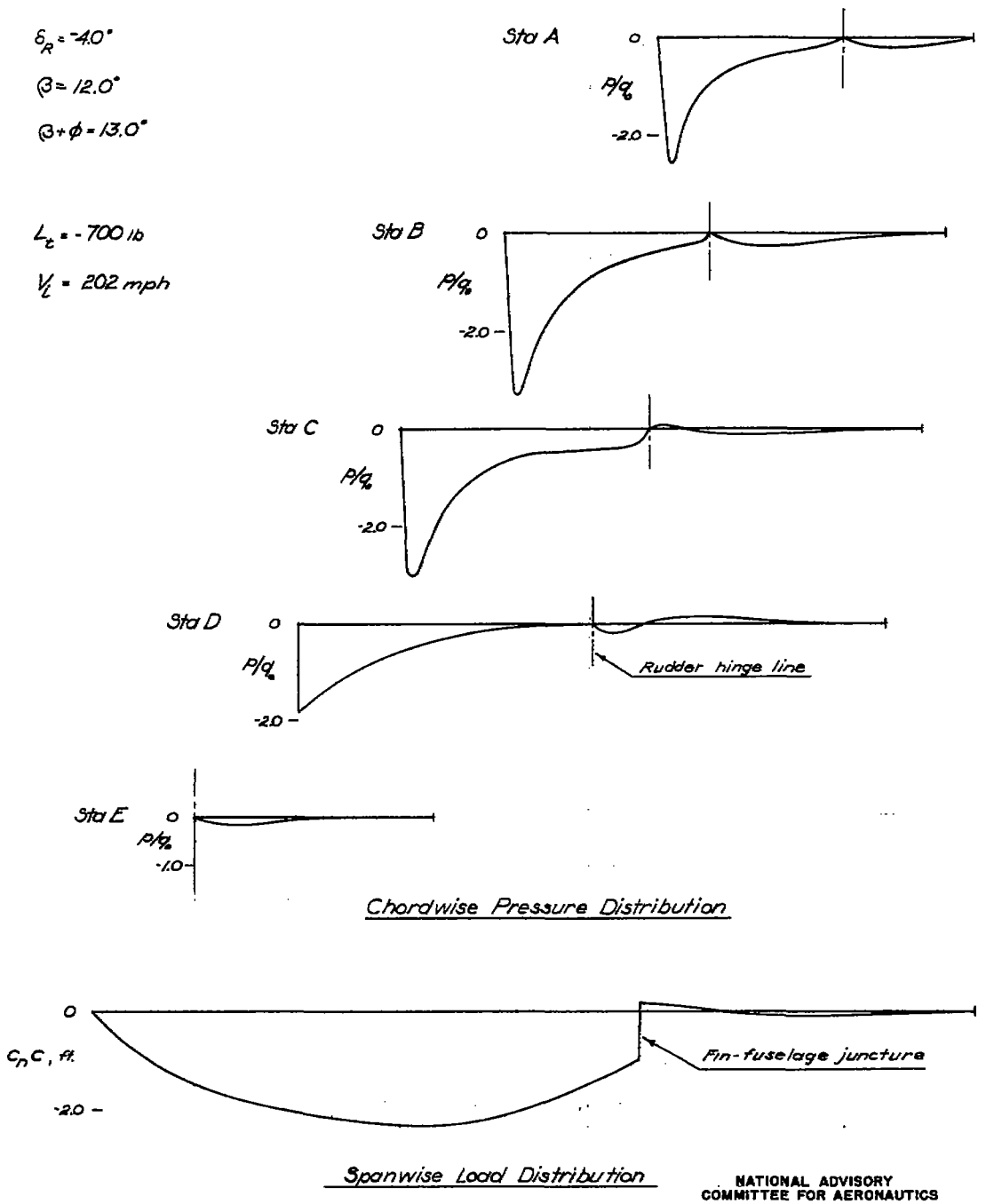

(b) Rolling-pullout maneuver

Figure 3.– Continued.

$\delta_R = -3.0°$

$\theta = 12.0°$

$\theta + \phi = 13.0°$

$L_t = -680$ lb

$V_t = 227$ mph

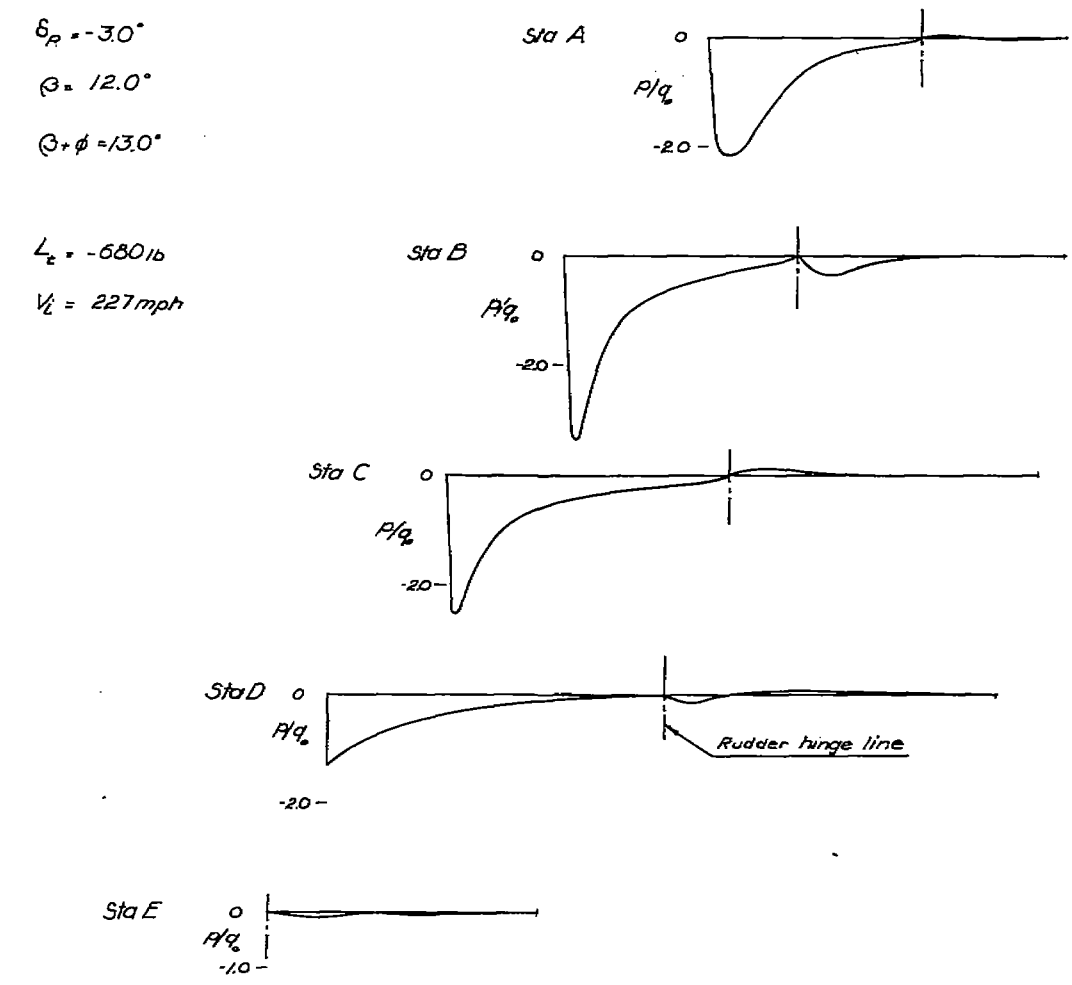

Chordwise Pressure Distribution

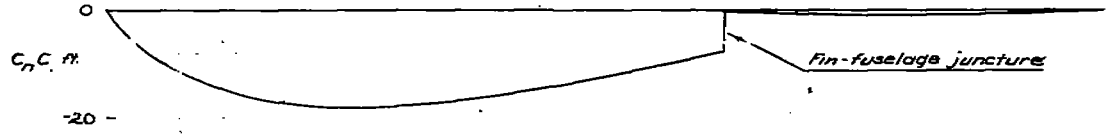

Spanwise Load Distribution

NATIONAL ADVISORY COMMITTEE FOR AERONAUTICS

(c) Fishtail maneuver

Figure 3.- Concluded.

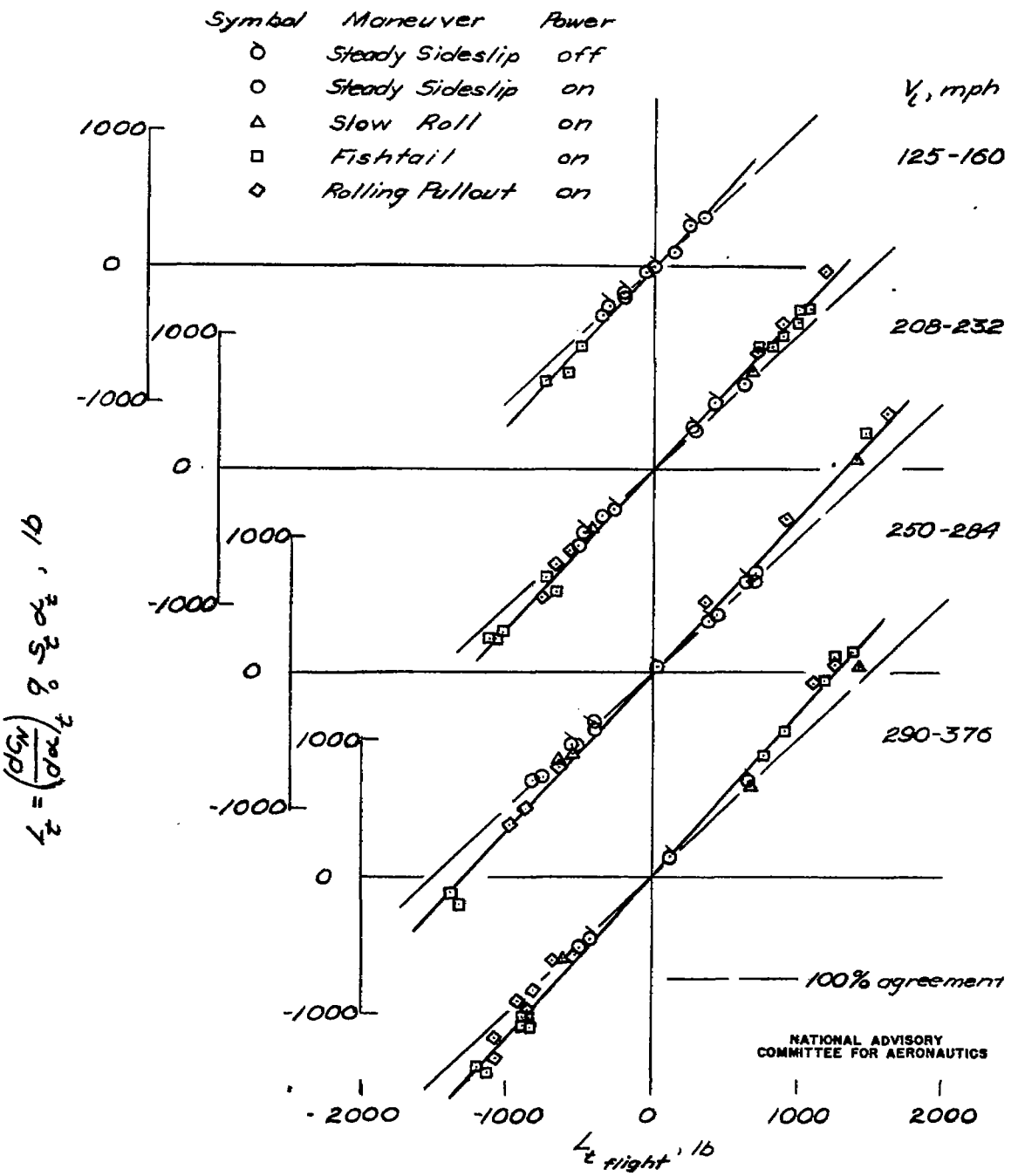

(a) $T_c = .74$

Figure 4.- Comparison of calculated vertical-tail loads and flight-measured vertical-tail loads at various airspeeds.

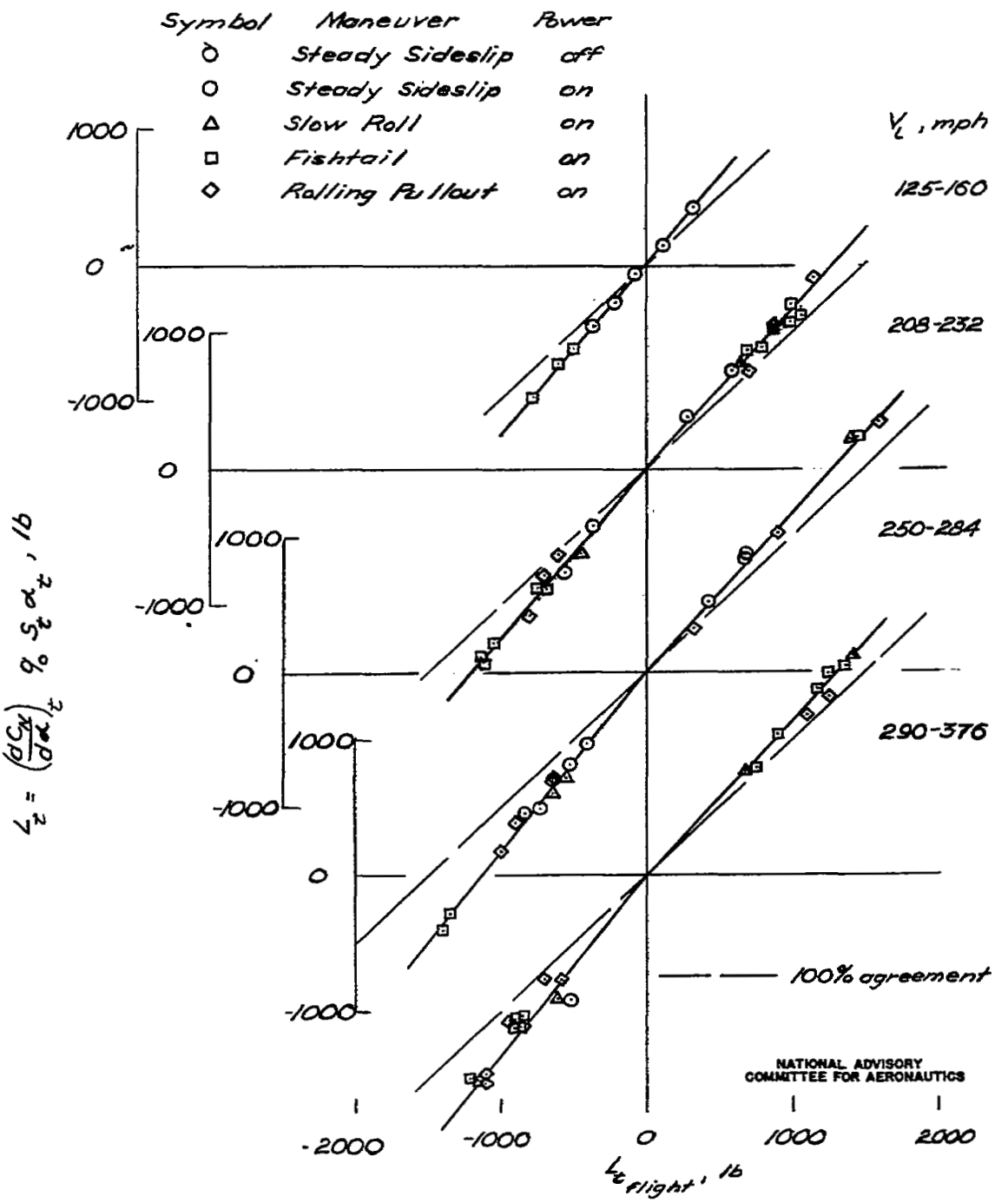

(b) $T_c = .50$

Figure 4.- Concluded.

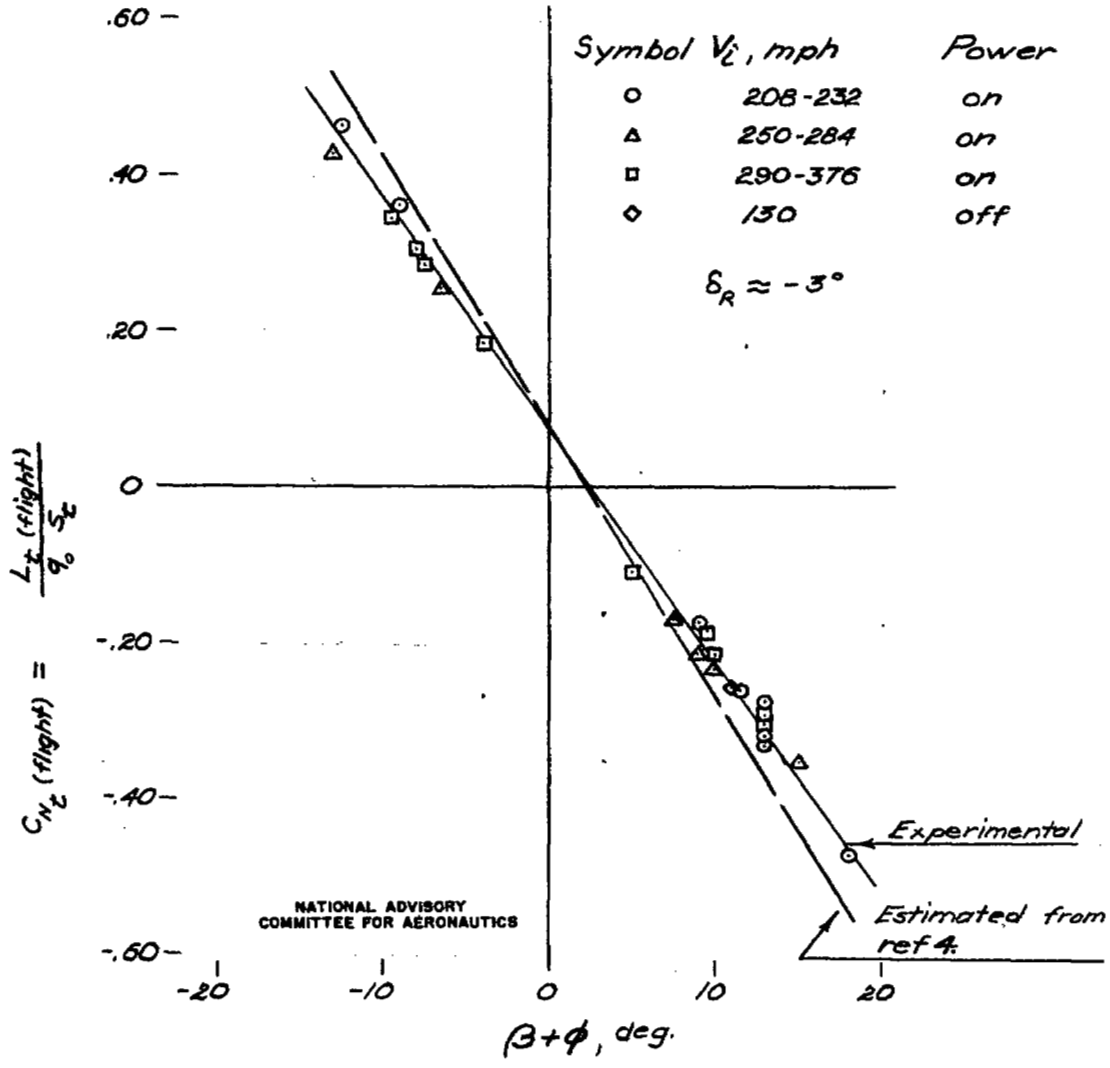

Figure 5:- Comparison of estimated and experimental vertical-tail lift curves at various indicated airspeeds in static and dynamic maneuvers.

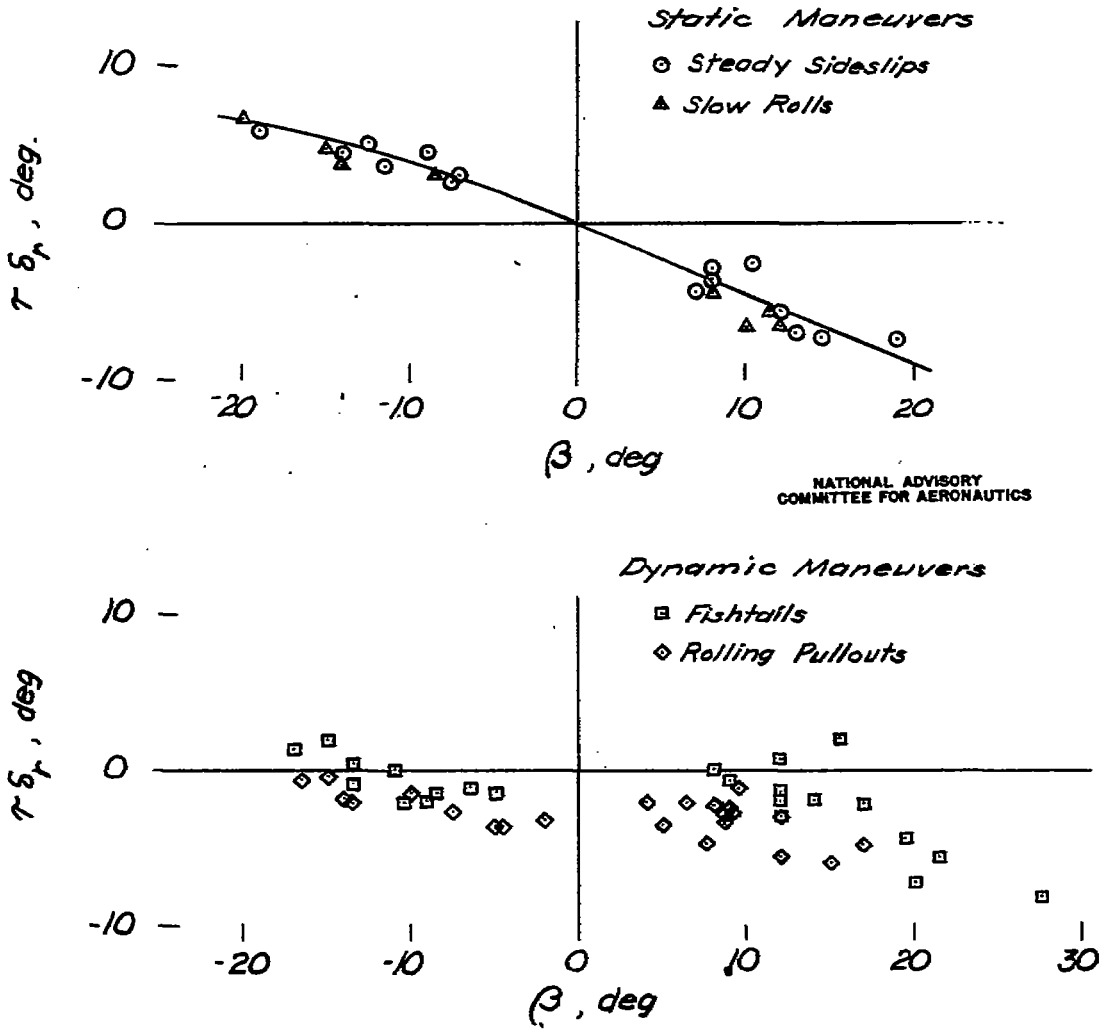

Figure 6.- Comparison of vertical-tail angle of attack increments due to rudder deflection with maximum sideslip angle; power on, $\tau = .74$.